THE BELL SYSTEM TECHNICAL JOURNAL
Vol. 58, No. 2, February 1979
Printed in U.S.A.

A New and Interesting Class of Limit Cycles in Recursive Digital Filters

By V. B. LAWRENCE and K. V. MINA

(Manuscript received February 1, 1978)

Limit cycles oscillations often occur in recursive digital filters due to the quantization of products in the feedback section. A new and interesting class of limit cycles has been discovered and categorized for second-order sections that round either sign-magnitude or twos-complement products. These limit cycles are named rolling-pin limit cycles. They are completely defined by three integers and a simple construction rule and exist for $B_1 - B_2$ pairs lying within small rectangular regions in the $B_1 - B_2$ (coefficient) plane. Each set of integers completely defines the peak amplitude, the length, and the region of existence. The amplitude of these limit cycles can be made close to but does not exceed three times the Jackson peak estimate. Rolling-pin limit cycles often occur in filters with high Q poles located near dc or half the sampling frequency. When these large amplitude limit cycles occur, the idle channel performance of a filter is often unacceptable. Specialized techniques, requiring extra circuitry, can be used to suppress them. Alternatively, it may be less costly and more efficient to avoid the small rectangular regions within which the rolling-pin limit cycles exist in the $B_1 - B_2$ coefficient plane.

I. INTRODUCTION

Oscillations often occur in recursive digital filters as a result of the nonlinear action of quantizing the products in the feedback sections. These oscillations occur in the least significant bits of the data and are called limit cycles.* These limit cycles influence the required internal data word length and hence the cost of the filter.[1]

This paper describes a new and important class of limit cycles that exist in second-order recursive digital filters. These limit cycles often occur in filters with high Q poles located near dc or half the sampling

* These limit cycles are to be distinguished from the large limit cycles caused by overflow.

frequency. They are called rolling-pin limit cycles and derive this name from their characteristic shape when plotted in the successive value plane (Fig. 2a). The second-order section under consideration employs rounding of both feedback products in either sign-magnitude or twos-complement number format and is shown in Fig. 1. The rolling-pin limit cycles are defined by three integers, K, L, and M, and a simple construction rule. As seen in Fig. 2b, K is the constant step size in the bandle of the rolling pin, L is the constant step size in the body of the rolling pin, and M is the number of steps of step size L. For each value of K, L, M, a unique set of limit cycles is completely defined. In this paper, emphasis is on the simplest case of $K = 1$.

This class of rolling-pin limit cycles is important because of its unusually large amplitude. Unusually large amplitude limit cycles can lead to severe distressing tones in idle channel conditions. It will be shown that the peak amplitude approaches three times Jackson's peak estimate.* The concept of regions of the $B_1 - B_2$ plane within which complicated limit cycles exist is important. The existence of these isolated areas within which tbe various K, L, M limit cycles exist presents an interesting "patchwork quilt" look in the $B_1 - B_2$ plane. A point of practical importance to note is that a small change in binary coefficient values (producing a pair of coefficients just outside the region of existence of rolling-pin limit cycles) can result in a 3:1 reduction in ac limit cycle amplitude. By ac limit cycles, we mean limit cycles with period >2.

Specialized techniques requiring extra circuitry[2-6] can be used to suppress rolling-pin limit cycles. These specialized techniques may increase the roundoff noise in the presence of a signal. Alternately, it may be less costly and more efficient to avoid rolling-pin limit cycles altogether, by avoiding the small rectangular regions within which they exist in the $B_1 - B_2$ (coefficient) plane.

In the sections that follow, we develop the explicit formulas for the peak amplitude, length, and regions of existence for the 1, L, M rolling-pin limit cycles. The various amplitude bounds and estimates that have been derived[7-12] in the past are examined relative to our exact peak values. A spectral analysis of rolling-pin limit cycles is also presented. A comparison of the roundoff noise and limit cycle power of a second-order section is made.

II. PROPERTIES OF *1, L, M* ROLLING-PIN LIMIT CYCLES

It is important to get an overall view of the nature of this class of limit cycles before examining tbeir detailed properties. For each value of L, M (the 1 will be omitted bereafter), a known number of rolling-pin limit cycles exist with identical bodies but handles that differ in

* Jackson's estimate (Ref. 7) is the integer part of $[0.5/(1 - B_2)]$.

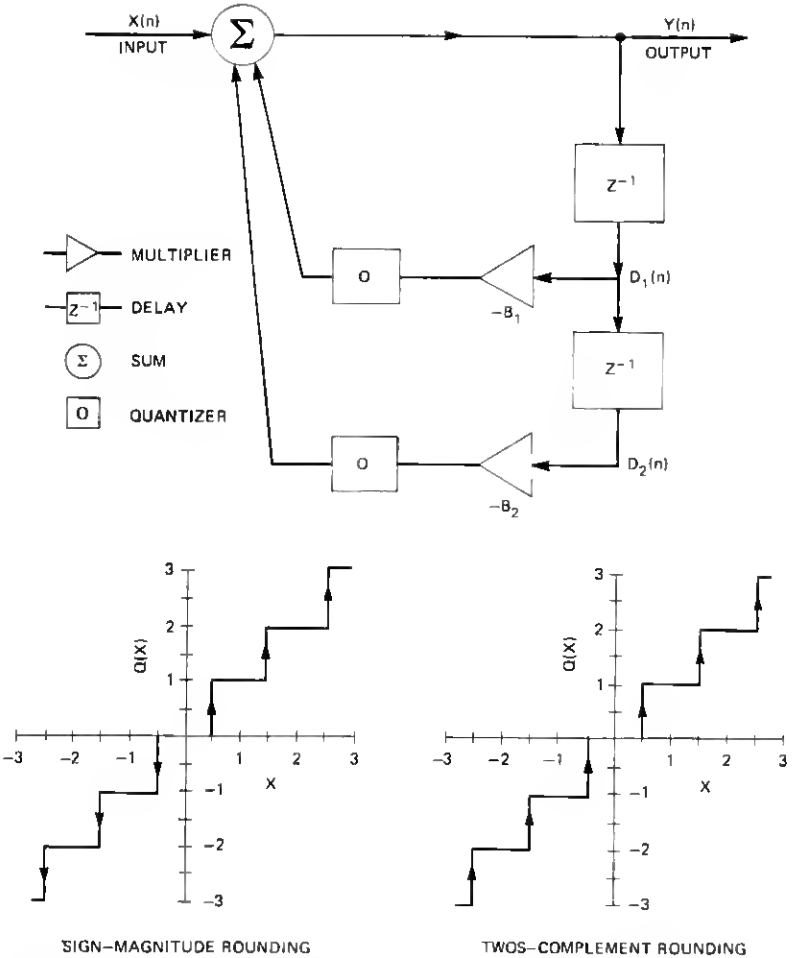

Fig. 1—(a) Second order pole section. (b) Quantization characteristics.

amplitude by one and overall length by four. For example, with $L, M = 3, 4$, there are three rolling-pin limit cycles with identical bodies but different peak amplitudes of 13, 14, and 15 and overall lengths of 34, 38, and 42, respectively. The successive value plane plots (hereafter called the $D_1 - D_2$ plots) for these three limit cycles are shown in Fig. 3. Each has its own cell of existence in the $B_1 - B_2$ plane. The three cells are horizontally contiguous as shown in Fig. 4. The boundaries on B_2 are

$$1 - (1/2)(1/9) > B_2 \geq 1 - (1/2)(1/8), \tag{1}$$

and on B_1 are

$$2 - (3/2)(1/15) > |B_1| \geq 2 - (3/2)(1/14) \text{ (amplitude 15)}$$

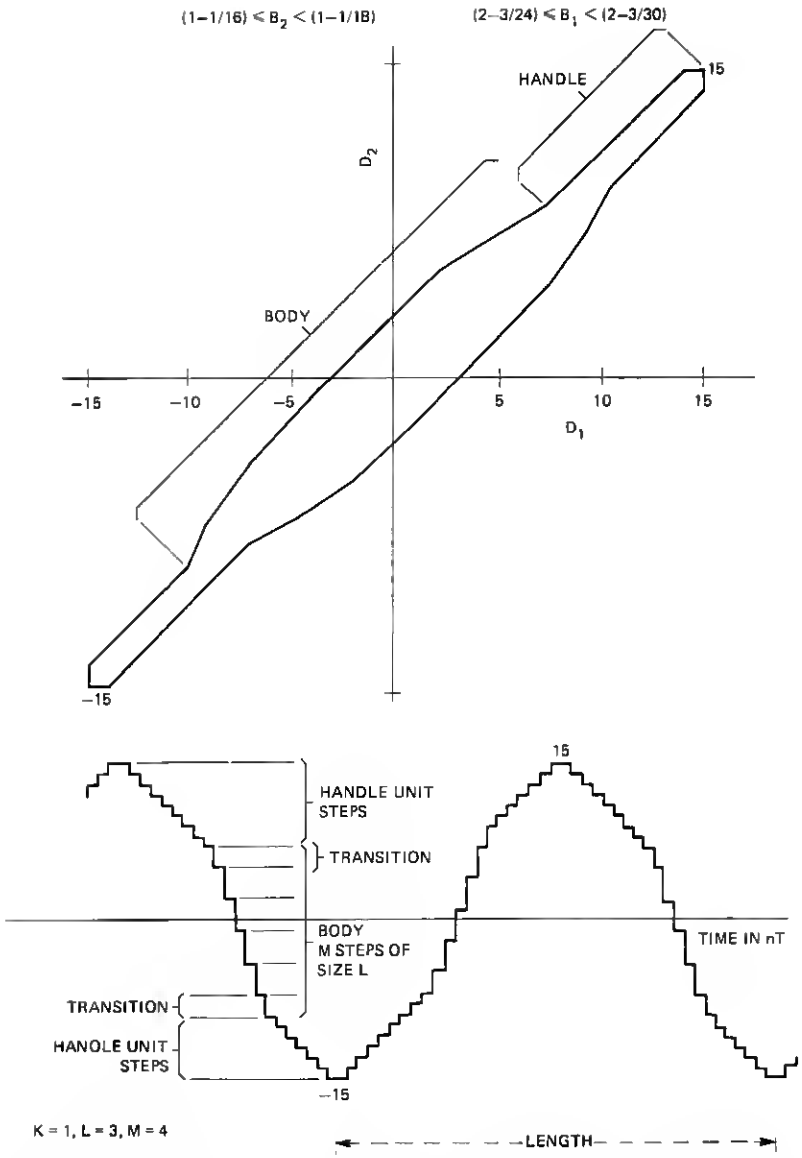

Fig. 2—(a) Successive value ($D_1 - D_2$) plot. (b) Time sequence for $K, L, M = 1, 3, 4$.

$$2 - (3/2)(1/14) > |B_1| \geq 2 - (3/2)(1/13) \text{ (amplitude 14)}$$
$$2 - (3/2)(1/13) > |B_1| \geq 2 - (3/2)(1/12) \text{ (amplitude 13).} \quad (2)$$

In Fig. 4, only negative values of B_1 (low-frequency poles) are shown; however, positive values of B_1 also produce related[12] limit cycles. For convenience, we shall emphasize negative values of B_1. The boundaries

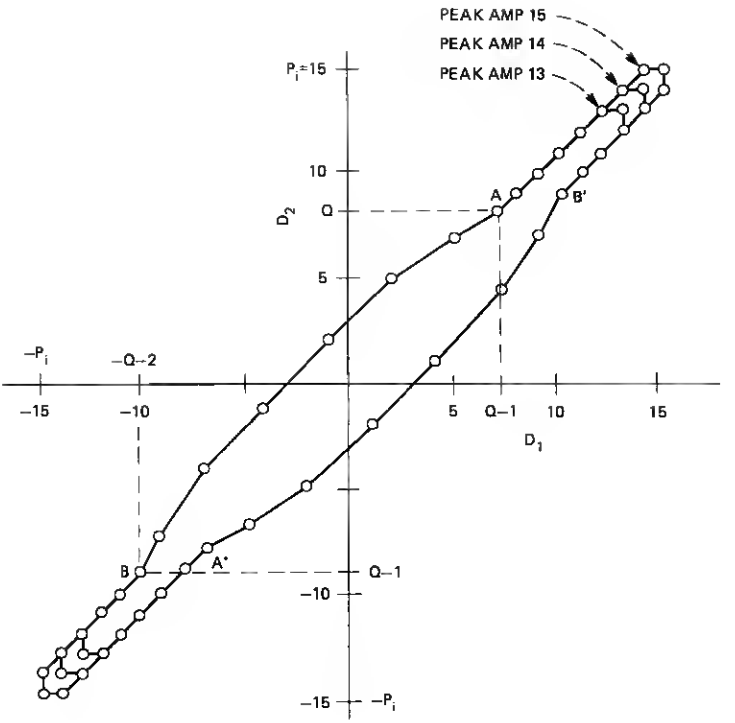

Fig. 3—Successive value ($D_1 - D_2$) plot for $L, M = 3, 4$.

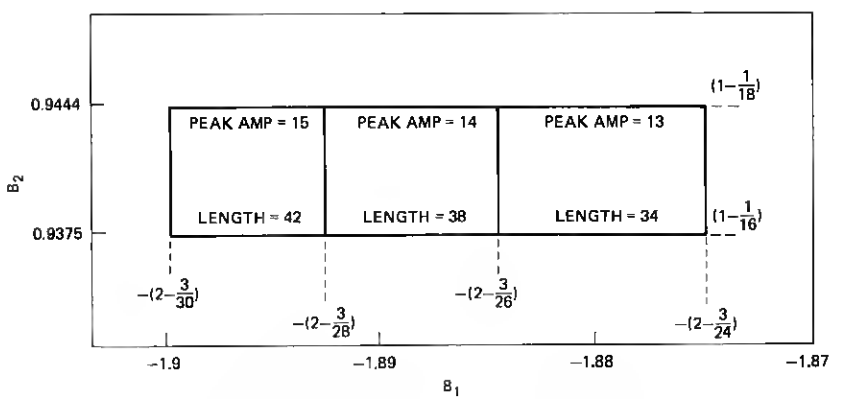

Fig. 4—Region of existence ($B_1 - B_2$ plane) for $L, M = 3, 4$.

defined in eqs. (1) and (2) are rational decimal (and rarely binary) numbers; however, in any implementation, the coefficients are binary. Accordingly, the equality signs in these constraints are usually not applicable.

For other values of L, M, similar sets of nearly identical limit cycles

exist with either $3(L-2)$ or $3(L-3)$ contiguous cells of existence depending on whether the product L, M is even or odd. For each L there is a minimum value of M (but no maximum value) below which a type of degeneracy occurs in which the handle disappears into the body. Figure 5 shows the regions in the $B_1 - B_2$ plane for which each set exists for $L = 3, 4, 5, 6$ and four values of M for each L. In each case, the boundaries on B_2 are of tbe form:

$$1 - 1/[2(Q+1)] > B_2 \geq 1 - 1/(2Q), \tag{3}$$

and the boundaries on B_1 are

$$2 - 3/(2P_i) > |B_1| \geq 2 - 3/(2P_{i-1}) \tag{4}$$

for $i = 1, 2, \cdots, (L-2)$ or $(L-3)$. Both Q and P_i are defined in terms of L and M in Section III. P_i is the peak amplitude of the limit cycle. The allowed B_1 and B_2 values always correspond to complex conjugate poles. This can be proved using eqs. (3), (4), (6), and (12).

Whenever either B_2 or B_1 is varied so that the outer boundary of a set of limit cycles is crossed, the rolling-pin limit cycle disappears and is replaced by a "normal" ac limit cycle with a smaller amplitude. The magnitude of the limit cycle is predicted by Jackson's estimate.[7] This effect should be borne in mind during the design of recursive filters, as an infinitestimal (binary) change in coefficient (and hence transfer function) can result in dramatic changes in the ac limit cycle properties. However, dc limit cycles larger than Jackson's estimate can still exist.

This class of limit cycles has the unique feature that, given L, M, all states and properties are completely defined. In the following sections, the construction rules for rolling-pin limit cycles are given and formulas are derived for their peak amplitudes, length, and $B_1 - B_2$ boundaries in terms of L and M.

III. CONSTRUCTION RULES FOR L, M ROLLING-PIN LIMIT CYCLES

The construction rules for rolling-pin limit cycles are best understood by reference to Fig. 6, where a time sequence of an arbitrary rolling-pin limit cycle is shown. The 1, L, M rolling-pin limit cycles have amplitudes with half-period odd symmetry, i.e.,

$$Y\left(n + \frac{N}{2}\right) = -Y(n), \tag{5}$$

where N is the period (or length) of the limit cycle and is an even number. The rules differ slightly for even and odd values of the product L, M; thus they are discussed separately.

3.1 Even L, M

As evident in Fig. 6, a rolling-pin limit cycle consists of sections of constant slope (i.e., constant first difference) separated by smooth

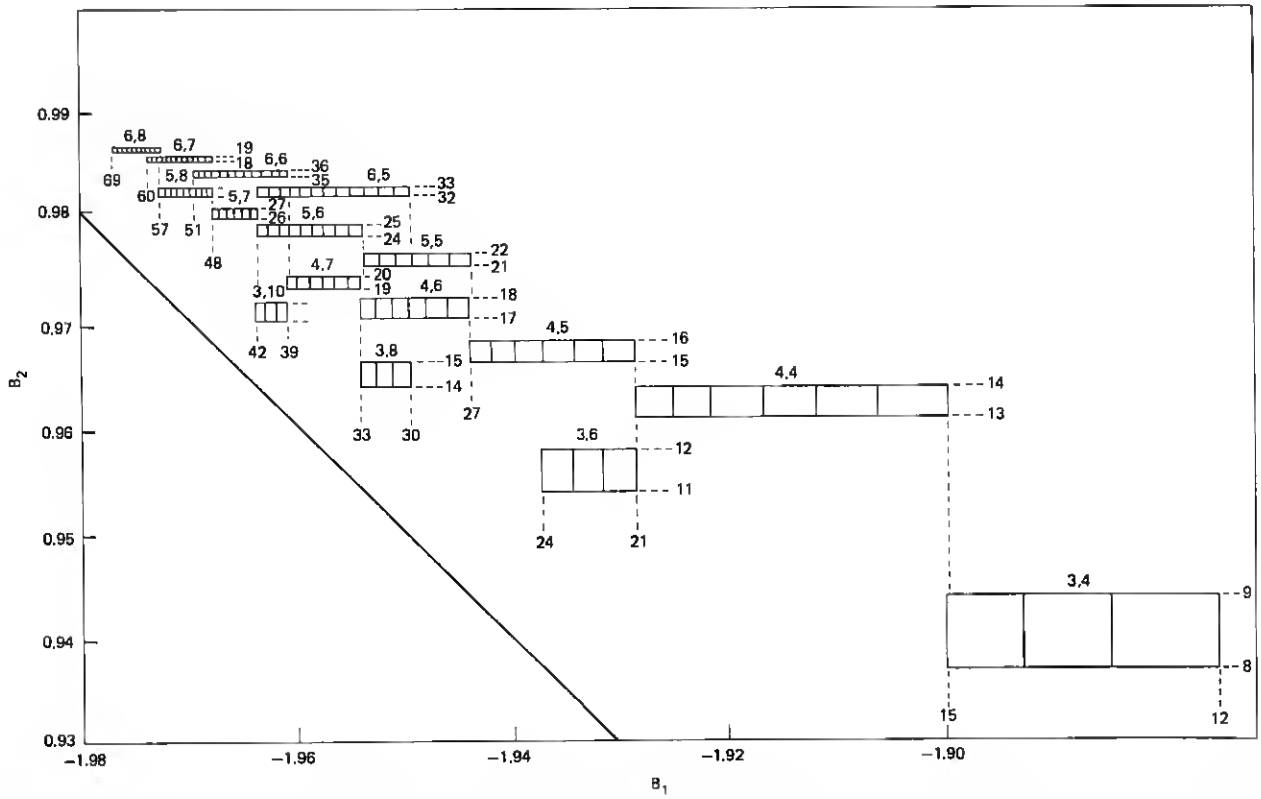

Fig. 5—Region of existence ($B_1 - B_2$ plane) for 4 sets of rolling-pin limit cycles. The bounds on B_1 are $2\text{-}3/(2i)$ and on B_2 $1\text{-}1/(2i)$ where the four appropriate values of i are shown by each rectangle.

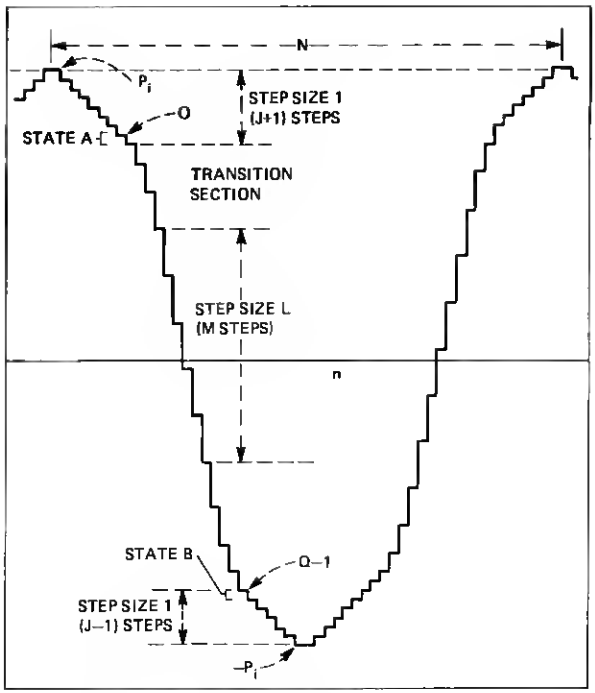

Fig. 6—Time sequence of 1, L, M limit cycle.

transition regions (of constant second difference). Due to the odd symmetry, we need consider only half a cycle of the time sequence. Starting from the positive peak, we find that a zero crossing occurs during the decreasing section of constant step size L. This section has exactly M steps and is preceded and succeeded by smooth transitions to sections of constant unit step size. The transition section is of length $L - 2$. The handle and the body of tbe rolling pin are pictorially obvious in the $D_1 - D_2$ plot in Fig. 2a; however, certain ambiguities arise in the discussion of the time sequence. First, every point in the $D_1 - D_2$ plot corresponds to a pair of values in the time sequence. Second, tbe transition region may be associated with either the handle or the body. The following convention will be used. The transition region is in the body of tbe rolling pin. The intersection of the handle and the transition region is also on the body. A value in the time sequence will be referred to as being on a certain part only when it is unambiguous. This would occur when both $D_1 - D_2$ points associated with the sample values were in the same part.

For a given L, M, the bodies of all the constituent limit cycles are identical. It is the handle that varies in amplitude. Any single point on the body can be used to start the construction. We choose a value, Q, which is associated with the intersection of the handle and the body

(state A in Fig. 7). This value Q, labeled in the time sequence in Fig. 6, is the next to last point on the unit step section immediately after the positive peak. For *all* even L, M,

$$Q = LM/2 + L(L-1)/2 - 1. \tag{6}$$

The point Q defines the B_2 bounds within which the limit cycle exists by

$$1 - \frac{1}{2(Q+1)} > B_2 \geq 1 - \frac{1}{2Q}. \tag{7}$$

Thus, for any even L, M we have defined the body of the rolling pin as well as the values of B_2 for which it exists. Continuing on the decreasing portion of the limit cycle, the intersection of the body and the handle reoccurs at point B in Fig. 7. The D_1, D_2 values of B are $-Q-2$, $-Q-1$. To verify this, we start at A, with $D_1^A = Q - 1$ and counting to B using the construction rule just outlined, we have

$$D_1^B = D_1^A - 2 - 3 \cdots - (L-1) - LM - (L-1) - (L-2) \cdots - 2 - 1$$

$$D_1^B = Q - 1\left(-2\sum_{i=1}^{L-1} i\right) + 1 - LM$$

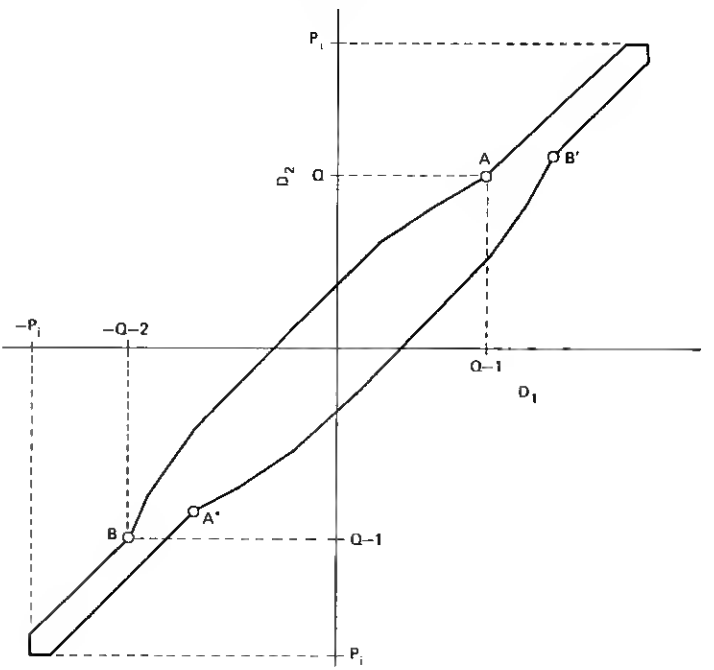

Fig. 7—$D_1 - D_2$ plot.

$$D_1^B = \frac{LM}{2} + \frac{L(L-1)}{2} - 2 - LM - L(L-1)$$

$$D_1^B = -LM - \frac{L(L-1)}{2} + 1 - 2$$

$$D_1^B = -Q - 2.$$

By symmetry, the states A' and B' also defined in Fig. 7 are $-Q + 1$, $-Q$ and $Q + 2$, $Q + 1$ respectively. For the case of $L, M = 3, 4$ (the smallest set of rolling-pin limit cycles), $Q = 8$ and the bounds on B_2 are

$$1 - 1/18 > B_2 \geq 1 - 1/16.$$

The common partial sequence in descending order is:

$$12, 11, 10, 9, \underbrace{\overset{Q}{8}, 7, 5, 2, -1, -4, -7,}_{\text{state } A} \quad \underbrace{-9, -10,}_{\text{state } B} \quad -11, -12.$$

Having defined the body, we now define the allowed lengths of the handle (which fixes the peak amplitude of the limit cycle) and the bounds on B_1. We do this by introducing the index J_i. J_i varies by unit steps from J_{max} to J_{min} inclusively, where

$$J_{min} = LM - \frac{L(L-1)}{2} - 3L + 5 \tag{8}$$

$$J_{max} = LM - \frac{L(L-1)}{2} - 2. \tag{9}$$

The peak amplitude of the limit cycle is given by

$$P_i = Q + J_i. \tag{10}$$

The number of nearly identical rolling-pin limit cycles is:

$$J_{max} - J_{min} + 1 = 3(L-2). \tag{11}$$

Equation (11) has to be positive for a rolling-pin limit cycle to exist; hence, the minimum value of L is 3. The range on the peak amplitude P_i is between P_{max} and P_{min}, where

$$P_{max} = Q + J_{max} = 3\left(\frac{LM}{2} - 1\right) \tag{12}$$

$$P_{min} = Q + J_{min}$$

$$= 3\frac{LM}{2} - 3L + 4. \tag{13}$$

For $L, M = 3, 4$

$$5 \leq J_i \leq 7$$
$$13 \leq P_i \leq 15.$$

The bounds on B_1 for each of the L, M rolling-pin limit cycles are

$$2 - \frac{3}{2P_i} > -B_1 \geq 2 - \frac{3}{2P_{i-1}} \quad \text{for} \quad i = 1, 2, \cdots, 3(L-2), \tag{14}$$

where

$$P_i = P_o + i \tag{15}$$

and

$$P_o = 3(LM/2 - L + 1). \tag{16}$$

Crossing either the bounds on B_2 or the outer bounds on B_1 results in elimination of the rolling-pin limit cycle. The amplitude of the resulting largest ac limit cycle will then be predicted by the Jackson estimate.

The length of the limit cycle is N, where

$$N = (4J_i + 4L - 6 + 2M). \tag{17}$$

Since N contains the term $4J_i$ and J_i varies by 1 for each sucessive limit cycle in the set, N varies by 4.

The example used throughout this section has been for $L, M = 3, 4$ (the smallest of the set of the rolling-pin limit cycles). An example of a larger rolling-pin is $L, M = 7, 8$. This set has $3(L-2) = 15$ possible rolling-pin limit cycles. The peak amplitudes vary from 67 to 81. The values of Q and P_o are 48 and 66 respectively. The index J_i varies from 19 to 33. Figure 8 shows a magnified portion of the $B_1 - B_2$ plane where this set exits, and in Fig. 9 the time sequence of the largest and smallest constituent limit cycles are tabulated.

3.2 Summary of construction rules and properties of the rolling-pin limit cycles

3.2.1 Even L, M

The results for even L, M rolling-pin limit cycles can be summarized as follows:

(*i*) There are $3(L-2)$ distinct limit cycles for any even L, M. Each has a time sequence with a half-period odd amplitude symmetry

$$Y\left(n + \frac{N}{2}\right) = -Y(n).$$

(*ii*) On the descending* half of the time sequence, there are
- (*a*) $J_i + 1$ steps of unit step size.
- (*b*) A smooth transition region (i.e., constant second difference).

* I.e., we start from the positive peak and scan the limit cycle.

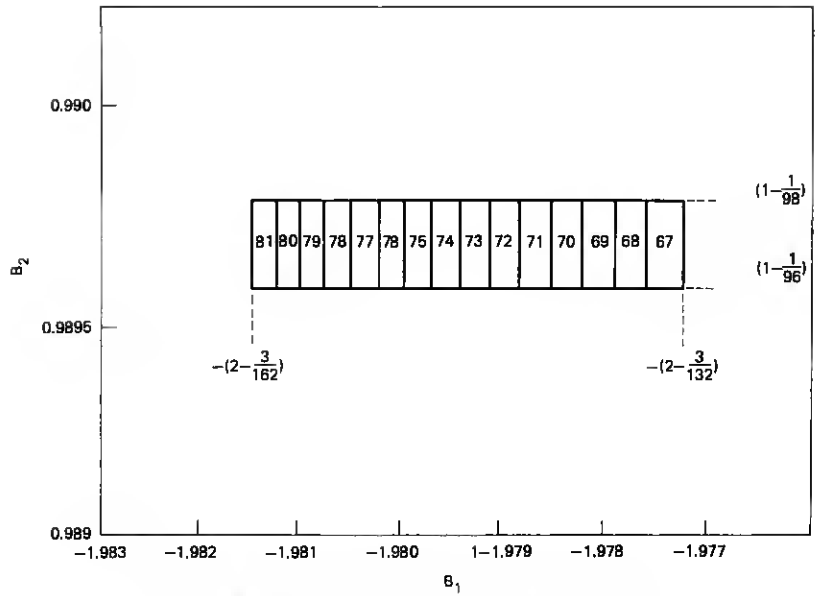

Fig. 8—Region of existence ($B_1 - B_2$ plane) for $L, M = 7, 8$.

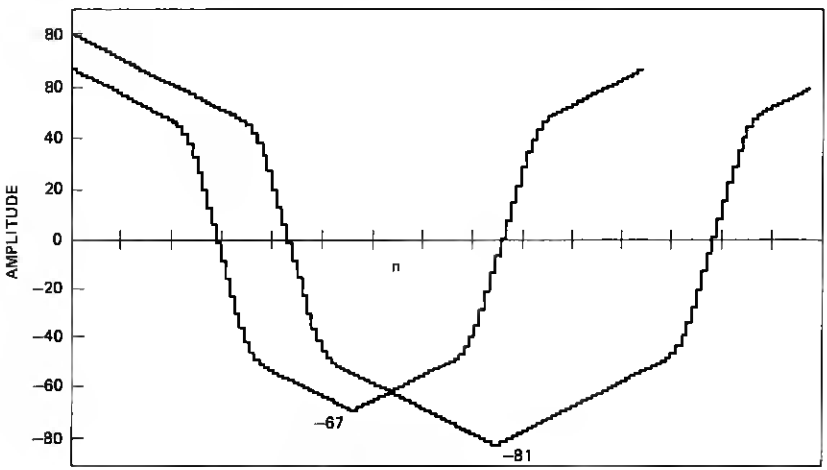

Fig. 9—Time sequences of $L, M = 7, 8$.

(c) M steps of step size L.
(*d*) A smooth transition region (also constant second difference).
(*e*) $J_i - 1$ steps of unit step size.

(*iii*) The peak amplitudes of the limit cycles are given by

$$P_i = J_i + Q,$$

where

$$Q = LM/2 + L(L-1)/2 - 1,$$

$$J_{\min} = LM - L(L-1)/2 - 3(L-2) - 1,$$

$$J_{\max} = LM - L(L-1)/2 - 2.$$

(*iv*) The region of existence of even L, M rolling-pin limit cycles in the $B_1 - B_2$ plane is defined by:

$$1 - \frac{1}{2(Q+1)} > B_2 \geq 1 - \frac{1}{2Q},$$

$$2 - \frac{3}{2P_i} > -B_1 \geq 2 - \frac{3}{2P_{i-1}} \quad \text{for} \quad i = 1, 2, \cdots, 3(L-2),$$

$$P_i = P_o + i,$$

where

$$P_o = 3(LM/2 - (L-2) - 1).$$

3.2.2 Odd L, M

Similar construction rules and bounds on B_1 and B_2 exist for odd values of L, M. These are simply summarized below.

(*i*) There are $3(L-3)$ distinct limit cycles for any odd L, M. Each has a half-amplitude period odd symmetry,

$$Y\left(n + \frac{N}{2}\right) = -Y(n).$$

(*ii*) On the descending half of the time sequence, there are
- (*a*) $J_i + 1$ steps of unit step size.
- (*b*) A smooth transition region (i.e., constant second difference).
- (c) M steps of step size L.
- (*d*) A smooth transition region (i.e., constant second difference).
- (*e*) $J_i - 2$ steps of unit step size.

(*iii*) The peak amplitude of the limit cycle is given by

$$P_i = J_i + Q,$$

where

$$Q = (LM-1)/2 + L(L-1)/2 - 1 \tag{18}$$

$$J_{\min} = (LM-1) - \frac{L(L-1)}{2} - 3(L-3) - 1 \tag{19}$$

$$J_{\max} = (LM-1) - \frac{L(L-1)}{2} - 2. \tag{20}$$

(*iv*) The region of existence of odd L, M rolling-pin limit cycles in the $B_1 - B_2$ plane is defined by

$$1 - \frac{1}{2(Q+1)} > B_2 \geq 1 - \frac{1}{2Q},$$

$$2 - \frac{3}{2P_i} > -B_1 \geq 2 - \frac{3}{2P_{i-1}},$$

for $i = 1, 2, \cdots, 3(L-3)$, where

$$P_i = P_o + i,$$

$$P_o = 3\left(\frac{(L\,M-1)}{2} - (L-3) - 1\right). \tag{21}$$

A point to note is that, for an odd L, M rolling-pin limit cycle to exist, we must have $L \geq 5$.

The length of the limit cycle is N where

$$N = (4J_i + 4L + 2M - 8). \tag{22}$$

Comparison of the equations for L, M odd with the equations for L, M even shows that the basic forms of the equations are identical if we interchange the following two quantities:

$$\frac{LM}{2} \leftrightarrow \frac{LM-1}{2}$$

$$3(L-2) \leftrightarrow 3(L-3).$$

An example of odd L, M for L, $M = 5, 7$ is given. A magnified portion of the region of existence of this set in the $B_1 - B_2$ plane is shown in Fig. 10. The time sequences of the largest and smallest members of this set are tabulated in Fig. 11.

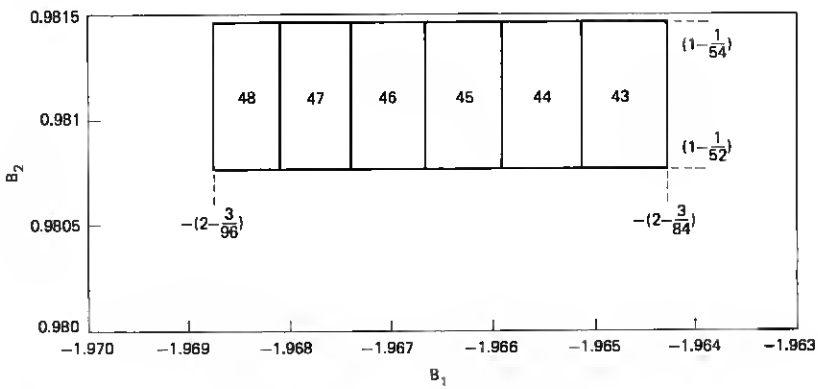

Fig. 10—Region of existence of L, $M = 5, 7$.

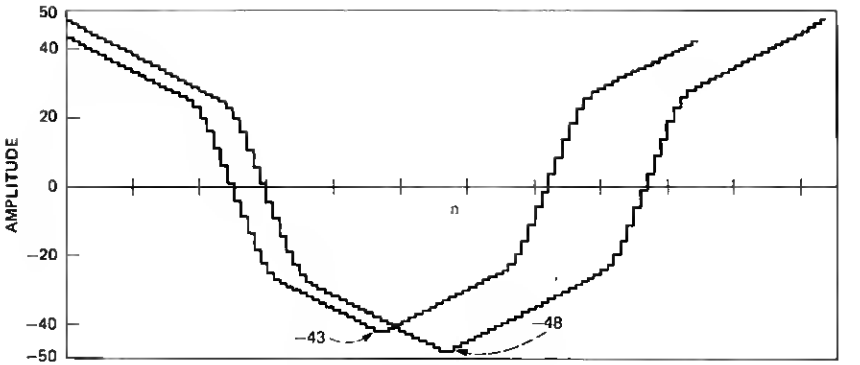

Fig. 11—Time sequences of L, $M = 5, 7$.

IV. ADDITIONAL PROPERTIES OF *1,L,M* LIMIT CYCLES

4.1 Peak amplitude comparisons

In this section, the ratio, ρ, of the peak amplitude of a rolling-pin limit cycle and Jackson's peak amplitude estimate[7] are determined. In addition, the actual peak amplitudes of the L, $M = 3, 4$ and L, $M = 3, 12$ rolling-pin limit cycles are compared to other calculated amplitude bounds or estimates.[7-11]

The peak amplitude of all rolling-pin limit cycles exceeds Jackson's estimate. It is now shown that the peak amplitude of a rolling-pin limit cycle approaches three times Jackson's estimate.* For convenience, we consider only even L, M.

Jackson's estimate is

$$JE = \frac{1}{2} \cdot \frac{1}{(1 - B_2)}. \tag{23}$$

Since this depends only on B_2, we can maximize ρ by minimizing JE. To do this, we pick the smallest value of B_2 that will cause the rolling-pin limit cycle to occur. This value is given by

$$B_2 = 1 - \frac{1}{2Q}, \tag{24}$$

so that

$$JE = Q = \frac{LM}{2} + \frac{L(L-1)}{2} - 1. \tag{25}$$

For a given L, M and a fixed $B_2 = 1 - 1/2Q$, a set of rolling-pin limit cycles exist. To maximize ρ we pick the largest amplitude case [eq. (12)],

* Parker and Hess conjectured in Ref. 8 that the limit cycle amplitude bound is three times the Jackson estimate.

$$P_{\max} = 3\left(\frac{LM}{2} - 1\right). \tag{26}$$

Then

$$\rho = \frac{JE}{P_{\max}} = 3 \cdot \frac{1}{1 + \dfrac{L(L-1)}{LM-2}}. \tag{27}$$

For a fixed L, ρ may be made arbitrarily close to 3 by increasing M. For the two examples, $L, M = 3, 4$ and $L, M = 3, 12$, ρ is 1.875 and 2.55 respectively.

Table I shows a comparison of the peak amplitudes for rolling-pin limit cycles of $L, M = 3, 4$ and $L, M = 3, 12$ with the bounds and estimates given by various authors.[7-11] As seen in this table, the actual peak amplitude is far less than the bounds predicted in Refs. 8 to 11. The Lyapunov bound[8] is the most pessimistic. The Sandberg-Kaiser peak amplitude estimate is $\sqrt{2}/2$ times their rms bound.[9] It is the best estimate for these examples. But even this bound is a factor of 6 higher for $L, M = 3, 4$ and a factor of 14 higher for $L, M = 3, 12$.

4.2 Mean-square-value comparison

Since all the states of the 1, L, M limit cycles are known, it is possible to develop an exact expression for the mean square value of the limit cycle sequence. The resulting expression is unfortunately complicated. The exact mean square value will however be compared to the Sandberg-Kaiser mean square bound for a number of examples. We define the ratio γ,

γ = Sandberg-Kaiser rms bound/actual rms value for various values of L and M. The Sandberg-Kaiser rms bound is

$$SK = \left| \frac{1}{(1-B_2)\sqrt{1 - B_1^2/4B_2}} \right| \quad \text{if} \quad \frac{4B_2}{(1-B_2)} > B_1. \tag{28}$$

For $P_i = P_{\max}$, the above inequality on B_1 and B_2 reduces to

$$12Q > 4P + 3 \quad \text{or} \quad 2L(L-1) > 1, \tag{29}$$

which always holds for rolling-pin limit cycles. Using the values of B_1, B_2 in the lower left-hand corner of the rectangle where the limit cycle exists, we have

$$(SK)^2 = \frac{2(2P_i)^2(2Q)^2(2Q-1)}{6(2P_i)(2Q) - 9Q - 2(2P_i)^2}. \tag{30}$$

The ratio γ was calculated for the largest limit cycle in the set 1, L, M for values of $L = 4, 6, 8, 10$, and 12 and values of $M = M_{\min}$ to ($M_{\min}$

Table I—Comparison of various bounds, Refs. 7–11

L, M	Arbitrary Binary Coefficients Chosen Within the Cells	Actual Peak	Jackson's Peak Estimate[7]	Parker and Hess Peak Estimate[8]	Sandberg and Kaiser[9] RMS Bound	Sandberg and Kaiser[9] Peak Estimate	Long and Trick Bound[10]	Lyapunov Peak Bound[8]	Peak Bounds Requiring Knowledge of Length[10] Actual Length N	Peak Bounds Requiring Knowledge of Length[10] Length Using Angle of Pole
									($N = 34$)	($N = 25$)
$L = 3$ $M = 4$	$B_2 = 0.9375$ $B_1 = 1.875$	13	8	24	64	90	125	488	42	80
									($N = 38$)	($N = 29$)
$L = 3$ $M = 4$	$B_2 = 0.9375$ $B_1 = 1.890625$	14	8	24	74	104	145	648	55	94
									($N = 42$)	($N = 32$)
$L = 3$ $M = 4$	$B_2 = 0.9375$ $B_1 = 1.8984375$	15	8	24	81	114	159	776	64	101
									($N = 146$)	($N = 76$)
$L = 3$ $M = 12$	$B_2 = 0.9755859375$ $B_1 = 1.96875$	49	20	60	498	704	990	11.7×10^3	626	578
									($N = 150$)	($N = 82$)
$L = 3$ $M = 12$	$B_2 = 0.9755859375$ $B_1 = 1.969703125$	50	20	60	538	760	1069	13.6×10^3	629	685
									($N = 154$)	($N = 90$)
$L = 3$ $M = 12$	$B_2 = 0.9755859375$ $B_1 = 1.9705875$	51	20	60	585	827	1162	16×10^3	619	737

Note: For bounds which require knowledge of the length, the two Parker and Hess[8] matrix methods and the Long and Trick method[10] will produce similar results. In this table the Long and Trick method was used in calculating the peak bound. In calculating the length from information about the angle of the pole, we have made the assumption that the limit cycle has a fundamental frequency equal to the frequency that corresponds to the angle of the pole.

+ 10).* The results are plotted in Fig. 12. It can be seen that the *SK* rms bound is too high by a factor between 7 and 30. As either L or M is increased (the poles approach the unit circle), γ increases approximately linearly (pessimistically).

4.3 Comparison of roundoff noise and limit cycle power

In this section, the formula for the roundoff noise power from an isolated second-order section is derived in terms of P_i and Q. A comparison between this noise power and the limit cycle power is given for $L = 3$, 4, 5, and 6 and four values of M for each L. It is concluded from the results of the comparison that the limit cycle power is likely to dominate.

The average roundoff noise power at the output of the second-order filter section shown in Fig. 1 is given by

$$\sigma_R^2 = 2\frac{E_o^2}{12}\int H(Z)\cdot\overline{H(Z)}\frac{dz}{Z}. \tag{31}$$

$H(Z)$ is the transfer function of the second-order section. $\overline{H(Z)}$ is the complex conjugate of the transfer function. The quantization of products in the presence of a signal is modeled by two white noise sources and is accounted for by the $2E_o^2/12$ term where E_o is the quantization step size of the filter. Evaluating the contour integral of eq. (31), we obtain

$$\sigma_R^2 = 2\frac{E_o^2}{12}\frac{(1+B_2)}{(1-B_2)}\frac{1}{(1+B_2)^2-B_1^2}. \tag{32}$$

Expressing eq. (32) in terms of P_i and Q, we have

$$\sigma_R^2 = 2\frac{E_o^2}{12}(4Q-1)\frac{4P_i^2Q^2}{P_i^2(1-8Q)+3Q^2(8P_i-3)}. \tag{33}$$

The limit cycle power is defined as

$$\sigma_L^2 = E_o^2\sum_{i=1}^{N}\frac{D_i^2}{N}, \tag{34}$$

where D_i are the values of the limit cycle.

A useful comparison is to calculate

$$\beta = 10\log(\sigma_L^2/\sigma_R^2). \tag{35}$$

This gives an estimate of the relative importance of errors in the presence of a signal and errors in idle channel conditions. This is only an estimate, since the limit cycles have specific frequencies while the roundoff noise has a flat spectrum. In a cascade of sections, for

* $M_{\min}$ is the minimum value of M for which the rolling-pin limit cycles exist in their nondegenerate form. See Section V.

example, succeeding poles and zeros may completely eliminate or amplify one or more of the limit cycle frequencies. Spectral analysis of the rolling-pin limit cycles has been carried out. Figure 13 shows a typical result. These results indicate that several frequencies are present. Accordingly, the estimate β is likely to be useful. In Table II, the value of β in decibels is calculated for $L = 3, 4, 5$, and 6 and four values of M. In each case, the limit cycle noise power is larger. On the

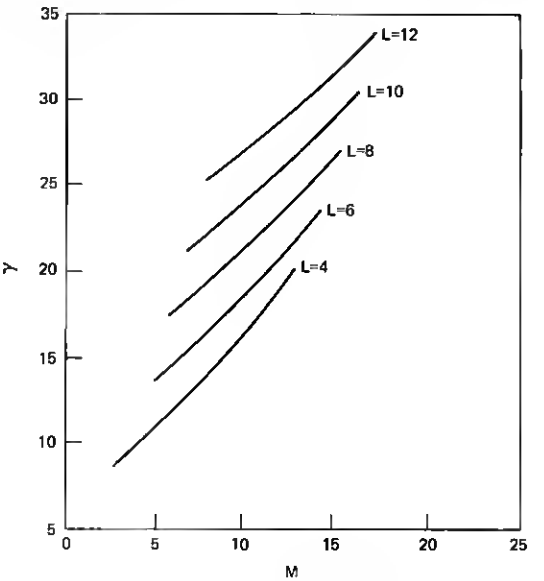

Fig. 12—Ratio of rms bounds.

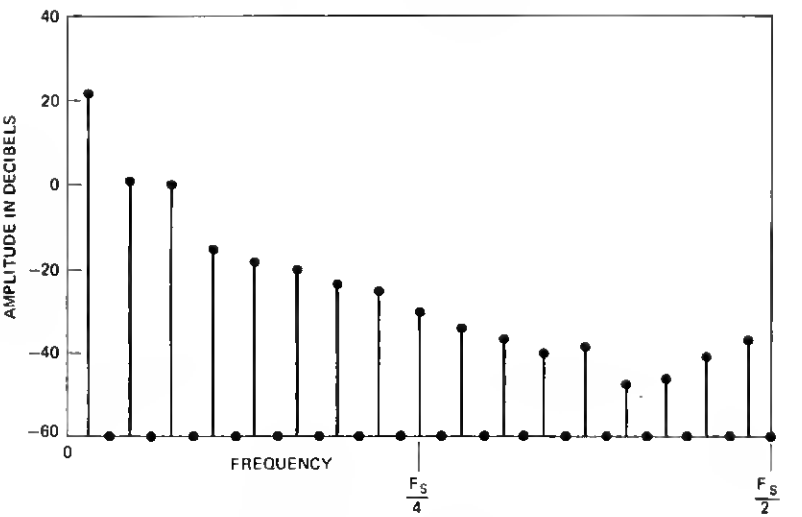

Fig. 13—Spectra of limit cycle.

Table II—Comparison of roundoff noise power and limit cycle power for various values of L, M

L, M	Roundoff Noise Power σ_R^2	Limit Cycle Power σ_L^2	$\beta = 10 \log \frac{\sigma_L^2}{\sigma_R^2}$ dB
3, 4	35.9	108.6	4.8
3, 6	108	264.8	3.9
3, 8	240.2	488.6	3.1
3, 10	450.3	780.1	2.4
4, 4	66.3	228.24	5.4
4, 5	113.1	365.5	5.1
4, 6	177.3	533.5	4.8
4, 7	261.5	732.4	4.5
5, 5	162.6	582.4	5.5
5, 6	269.8	915.8	5.3
5, 7	361.6	1173.3	5.1
5, 8	533.9	1624.9	4.8
6, 5	262.9	993.4	5.8
6, 6	388.2	1424.4	5.6
6, 7	545.9	1924.8	5.5
6, 8	739.6	2496.1	5.3

basis of these results, it is expected that limit cycle behavior will dominate in establishing the internal data word length of digital filters that generate rolling-pin limit cycles.

4.4 DC and tha amall ac limit cyclea

A number of dc and small ac limit cycles are produced by the same second-order sections that produce the rolling-pin limit cycles. These small ac limit cycles are not accessible in the sense of Claasen et al.[12] and their peak amplitudes do not exceed the Jackson estimate. The states and form of these small ac limit cycles can also be characterized by integers. Each of these small ac limit cycles has no handles. They only have a constant step-size body* with smooth transitional paths to their peaks. These smaller limit cycles can be constructed using the method outlined in Section V for rolling-pin limit cycles.

The total number of these small ac limit cycles is $(Q - P_o/3 - 1)$, where Q and P_o can be obtained from eqs. (6) and (16), respectively. The peak amplitude of the smallest ac limit cycle is $(P_o/3 + 1)$. The largest amplitude of the small ac limit cycles is $(Q - 1)$. For $L, M = 3, 4$ we have $Q = 8$ and $P_o/3 = 4$. Therefore, there are three small ac limit cycles. The smallest has a peak amplitude of 5 and the largest a peak amplitude of 7.

The $D_1 - D_2$ plot of all the small ac and dc limit cycles for $B_1 = -1.875$ and $B_2 = 0.9375$ (binary coefficients within the region for $L, M = 3, 4$) is shown in Fig. 14. The three large rolling-pin limit cycles are

* For these various small limit cycles, the constant step size ranges from 1, 2$\cdots$ $(L - 1)$, where L is the constant step size of the body of the associated rolling-pin limit cycle.

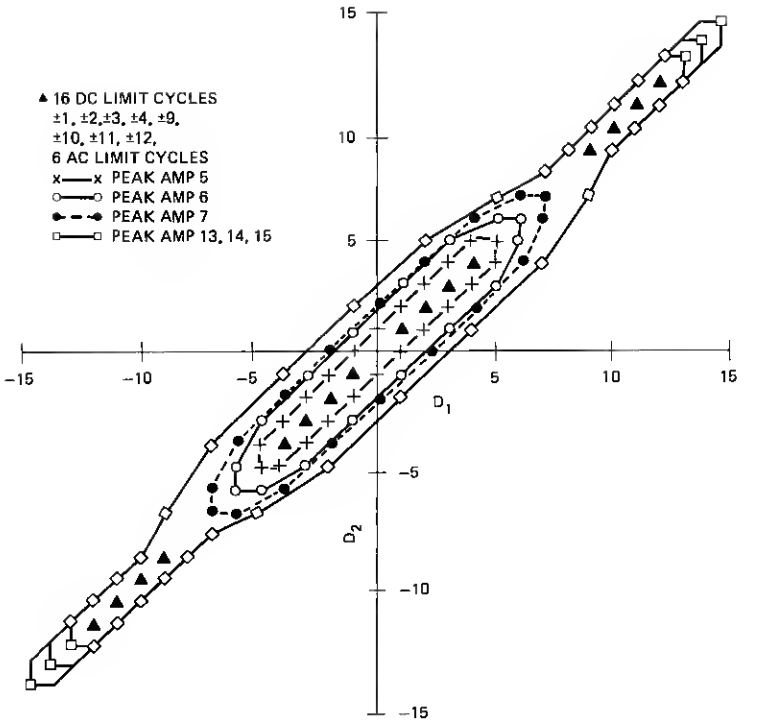

Fig. 14—Successive value ($D_1 - D_2$) plot small and large limit cycles.

also shown in Fig. 14. The regions of existence of these small ac limit cycles together with the three rolling-pin limit cycles are shown in Fig. 15. The rolling-pin limit cycles exist in a relatively smaller region. The small ac limit cycles exist in regions all the way up to the stability boundary $B_2 = 1$.* We see from Fig. 15 that, as the rolling-pin boundaries are crossed, the larger rolling-pin limit cycles disappear. However, the small ac and dc limit cycles still remain.

The number of small dc limit cycles can also be evaluated. This number is equal to $2P_o/3$. Any state which satisfies the equation

$$-\frac{P_o}{3} \leq D_1 = D_2 \leq \frac{P_o}{3} \tag{36}$$

is a dc state. These states represent the small dc limit cycles. The larger dc limit cycles can be evaluated from the following equation:

$$Q + 1 \leq D_1 = D_2 \leq P_o. \tag{37}$$

For $B_1 = -1.875$ and $B_2 = 0.9375$, we have $Q = 8$ and $P_o = 12$. Therefore, there are 8 small dc limit cycles, ±1, ±2, ±3, and ±4, all

* Other limit cycles may also exist in the region outside the region of the rolling-pin limit cycles. No inference should be drawn on the existence of other limit cycles.

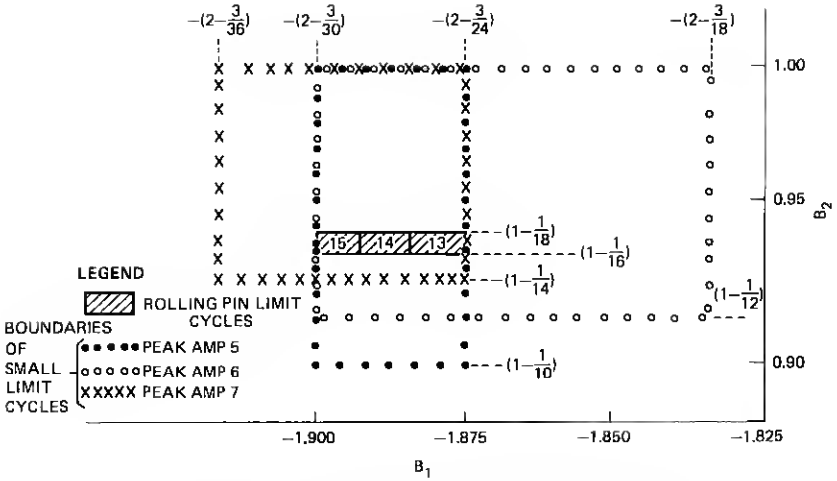

Fig. 15—Region of existence of small and large limit cycles.

satisfying eq. (36). In addition, there are 8 bigger dc limit cycles, ±9, ±10, ±11, and ±12. These values can be obtained from eq. (37). These 16 dc states are shown in Fig. 15. The state $\pm[Q, Q] = \pm[8, 8]$, which should normally correspond to the Jackson estimate is not on any limit cycle. The next state after the state ±[8, 8] is on a bigger limit cycle with peak amplitude 13. This state $\pm[Q, Q]$ is unique because it is a state from which one can spiral out onto a bigger limit cycle.

V. REGIONS OF EXISTENCE IN THE $B_1 - B_2$ PLANE

Each member of a set of rolling-pin limit cycles exists in a rectangular region. The boundaries of the regions are rational numbers. As seen in Fig. 5, the members within a set exist in horizontally contiguous regions. In any real implementation, the coefficients are binary. Strictly, all statements refering to regions of existence should refer to the binary valued points within (and occasionally on the boundary of) the regions. For simplicity, we refer only to the continuous regions to demonstrate why the regions are rectangular; we develop the explicit boundaries for rolling-pin limit cycles. We now construct the values of Q, J_i, and P_i, which were stated and used earlier. These variables, interestingly, depend on and follow from the assumed form of the body of the limit cycle which was constructed in Section III. The critical observation to make is that any state D_1, D_2 which generates the output Y [i.e., $(D_1, D_2) \rightarrow Y$] defines a region in the $B_1 - B_2$ plane. This region is an unbounded staircase of rectangles if $D_1 D_2 \neq 0$, or is a semi-infinite slab if D_1 or $D_2 \neq 0$. The rectangles for the case of (3, 2) $\rightarrow -1$ or $(-3, -2) \rightarrow 1$ are shown in Fig. 16. The height and width of each rectangle is $|1/D_2|$ and $|1/D_1|$, respectively. The center of each rectangle lies on the line defined by

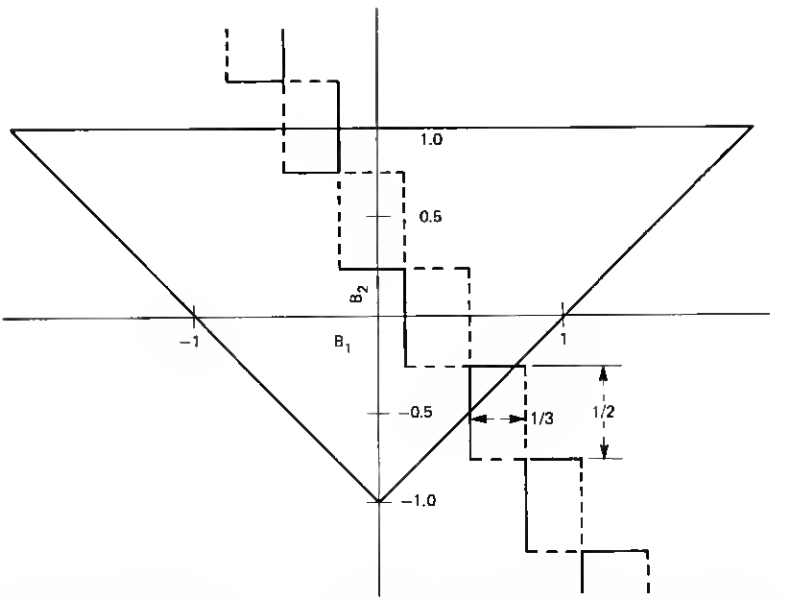

Fig. 16—Region of existence of a transition. Regions of existence include the solid, but not the dotted, boundary.

$$B_2D_2 + B_1D_1 = -Y, \tag{38}$$

with slope $-D_1/D_2$ and B_1 intercept $-Y/D_1$. The B_1 and B_2 intercepts of this line are both centers of rectangles. If $D_1 = 0$, there is a horizontal slab of height $|1/D_2|$ centered on $B_2 = -Y/D_2$. For $D_2 = 0$, there is a vertical slab of width $|1/D_1|$ centered on $B_1 = -Y/D_1$. This construction was done for sign-magnitude products for the circuit shown in Fig. 1. The rectangles include the solid boundaries but not the dotted boundaries since $\pm 1/2$ rounds to ± 1. For twos-complement rounding, the same figure applies with minor changes in the dotted and solid lines since, in twos-complement, $-1/2$ rounds to 0. Since any limit cycle is a sequence of transitions, the resulting region of existence is the region of the $B_1 - B_2$ plane common to all tbe transitions. This region must be a rectangle. (When independent stability arguments are applied, the stability triangle is superimposed, which may further reduce the common region. This is the only condition that can cause other than a rectangular region.)

Armed with this information, rolling-pin limit cycles were studied to determine the boundaries of their existence and to locate the critical transitions that set these boundaries. What was discovered was that the same transitions (relative to the overall shape of the successive value rolling-pin plot) *always* defined the $B_1 - B_2$ regions. Small differences exist depending on the evenness and oddness of L and M.

For convenience, we consider M even. Since for sign-magnitude rounding the states $(D_1, D_2) \rightarrow Y$ and $(-D_1, -D_2) \rightarrow -Y$ result in the same $B_1 - B_2$ region, we need only consider the half of the limit cycle from the positive peak to the negative peak. For M even, the state -1 always occurs on the limit cycle. The body of the limit cycle is symmetrical with respect to this -1 point. The critical transitions that set the B_2 boundaries are shown in Fig. 17a. Two transitions (T_u and T_u') set the maximum value of B_2 and one transition (T_L) sets the minimum value of B_2. The D_1 and D_2 states in these transitions are defined in terms of $Q = LM/2 + L(L - 1)/2 - 1$. The two transitions in the four consecutive states $Q + 1$, Q, $Q - 1$, $Q - 3$ completely determine the B_2 boundaries.

The boundaries on B_1 are more complex since a horizontally contiguous set of rectangles exist within each of which a separate rolling pin limit cycle occurs. The outer boundaries of this set of rectangles are determined by the two transitions T_u and T_L shown in Fig. 17b. The value of D_1 in the transition that sets the upper limit on B_1 is $-(1 + ML/2 - L)$. The value of D_1 in the transition that sets the lower limit on B_1 is $ML/2 - 1$. The inner B_1 boundaries that separate the nearly identical limit cycles in a set are fixed by the transitions at the peak of the limit cycle. Figure 17c illustrates this for a typical limit cycle in a set. As can be seen, the pair of consecutive transitions at either peak serves to set the inner boundaries on B_1. The peak transition of the largest limit cycle in the set sets the minimum bound on B_1. This

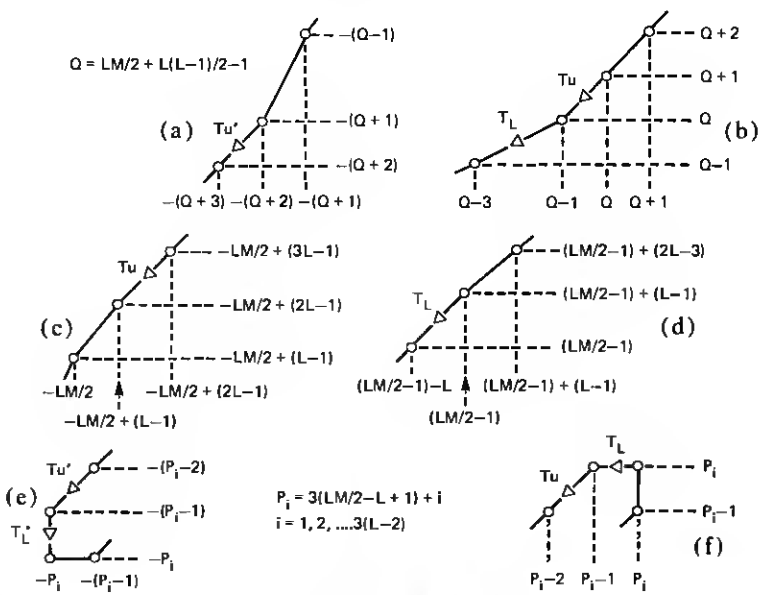

Fig. 17—Critical transitions.

bound is identical to the minimum bound on B_1 determined by the body. In fact, this is how the peak limit cycle of the set is defined. The peak transition of the smallest limit cycle in the set sets the maximum bound on B_1. This bound is identical to the maximum bound on B_1 determined by the body. All peaks are possible between and including these two. The number of limit cycles in the set is determined in this way.

When it is known which transitions set the boundaries and the values of the states in those transitions, the resulting boundaries are:

$$1 - \frac{1}{2(Q+1)} > B_2 \geq 1 - \frac{1}{2Q}$$

$$2 - \frac{3}{2P_{i+1}} > -B_1 \geq 2 - \frac{3}{2P_{i-1}}$$

for all $i = 1, 2, \cdots, 3(L-2)$, where i indexes the consecutive states and

$$P_o = 3\left(\frac{LM}{2} - L + 1\right).$$
$$P_i = P_o + i.$$

Since Q and P_i are integers, the boundaries are rational. The existence of the 2 in the denominator is expected since the boundaries must be associated with rounding products which are an integer $\pm 1/2$. The derivations of these boundaries is in principle possible by considering each transition in the body and locating a common region in the $B_1 - B_2$ plane. In practice, this is not accomplished; rather, the boundaries have been located using programming techniques. Insight into the process can be gained using the following approach. Assume for the critical B_1 transitions in the body that B_2 is effectively unity. (This must be rechecked later, but is in fact true.) The state equation for the circuit in Fig. 1 is then

$$-D_2 + \left| D_1\left(2 - \frac{1}{2X}\right) \right|_R = Y. \tag{39}$$

The subscript R signifies sign-magnitude rounding. For the lower B_1 bound, the values of D_1, D_2, Y are

$$\frac{LM}{2} + L - 2, \qquad \frac{LM}{2} - 1, \qquad \frac{LM}{2} - (L+1).$$

Using these values, eq. (39) becomes

$$\left| LM - 2 - \frac{1}{2X}\left(\frac{LM}{2} - 1\right) \right|_R = LM - 3.$$

This nonlinear equation due to the rounding is valid for the interval

$$\frac{3}{2} \geq \frac{1}{2X}\left(\frac{LM}{2} - 1\right) > \frac{1}{2}.$$

The lower B_1 bound corresponds to the minimum algebraic value of $[2 - (1/2X)]$ which occurs for the maximum value of $X = (LM/2) - 1$. This lower bound on B_1 is approachable but not attainable:

$$B_{1\,\text{lower}} = -2 + \frac{3}{2}\frac{1}{3\left(\frac{LM}{2} - 1\right)}.$$

In a similar fashion, the values of D_1, D_2, Y are

$$\left(2L - 1 - \frac{LM}{2}\right), \quad \left(L - 1 - \frac{LM}{2}\right), \quad \left(-1 - \frac{LM}{2}\right)$$

This transition leads to the attainable bound:

$$B_{1\,\text{upper}} = -2 + \frac{3}{2}\frac{1}{3\left(\frac{LM}{2} - L + 1\right)}.$$

Using a B_1 between these limits and considering the two transitions in Fig. 17a, the bounds on B_2 are found to be:

$$1 - \frac{1}{2(Q+1)} > B_2 \geq 1 - \frac{1}{2Q}.$$

Checking back on the assumption that B_2 is effectively unity, for $D_2 = -1 - \frac{LM}{2}$,

$$-\left|\left(1 - \frac{1}{2Q}\right)\left(-1 - \frac{LM}{2}\right)\right|_R = \left(-1 - \frac{LM}{2}\right) - \left|\frac{\left(1 + \frac{LM}{2}\right)}{2\left(\frac{LM}{2} + \frac{L(L-1)}{2} - 1\right)}\right|_{R'}.$$

Since the minimum L is 3, the R' operation yields a zero result and therefore B_2 is effectively 1. The R' operation is rounding except $\pm 1/2$ rounds to 0.

The quantity P_i is the peak value of the ith limit cycle. The remaining unknowns are $J_{\min}$ and $J_{\max}$. They follow from Q and P_i.

$$J_{\min} = P_1 - Q = LM - \frac{L(L-1)}{2} - 3\,(L-2) - 1$$

$$J_{max} = P_{3(L-2)} - Q = LM - \frac{L(L-1)}{2} - 2.$$

There are $J_{max} - J_{min} + 1 = 3(L-2)$ limit cycles in each set.

This discussion can be extended to the cases "M-odd, L-even" and "M-odd, L-odd." The minor differences that occur arise from the following. For "M-odd, L-even," the value $-L/2 - 1$ is on the body of the limit cycle. This, however, leads to no changes in the equations just developed. For "M-odd, L-odd," the value $-(L+1)/2 - 1$ is on the limit cycle. This causes the minor variations in the equations summarized in Section 3.3.

The final issue discussed in this section is a degeneracy that can occur for the smallest M for a given L. Essentially what happens is that the handle disappears into the body for some of the B_1 rectangles nearest the origin. To determine if degeneracy occurs, the equation for J_{min} must be examined. For a given L, since there are $J_i - 1$ steps in the negative handle, if $J_{min} > 1$, no degeneracy occurs. If $J_{max} > 1$, but J_{min} is not, degeneracy occurs for that value of M. Figure 18 shows a plot of J_{min} and J_{max} as a function of M for $L = 4$ and $L = 5$. As can be seen, degeneracy occurs for $L, M = 4, 3$ and $L, M = 5, 4$.

VI. GENERALIZED *K,L,M* ROLLING-PIN LIMIT CYCLES

Only the simplest class of rolling-pin limit cycles $(1, L, M)$ has been analyzed in this paper. Other classes exist with values of K larger than 1. The difference between the classes is K, which is the step size in the handle. The construction rules for the transition regions and the body are similar for all the classes. The other properties such as (*i*) regions of existence, (*ii*) peak amplitudes, (*iii*) mean square value, (*iv*) number

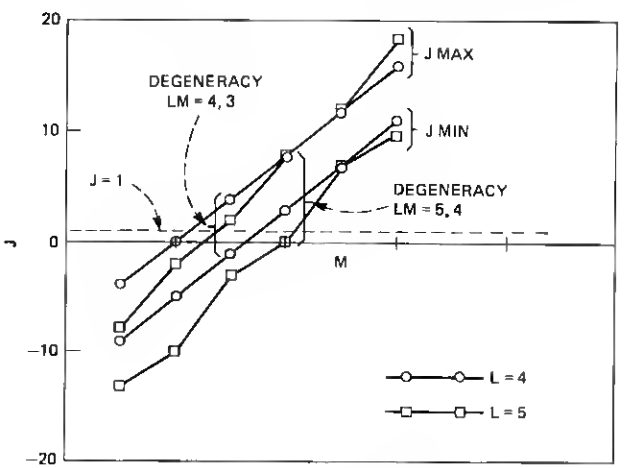

Fig. 18—Degeneracy criteria.

of cells, and (v) length can all be derived in terms of K, L, and M. The $D_1 - D_2$ plots, regions of existence, peak amplitudes, and number of cells for K, L, M =2, 6, 6 and K, L, M = 3, 8, 5 are shown in Figs. 19 and 20, respectively.

VII. CONCLUSIONS AND EXTENSIONS

A unique set of unusually large limit cycles has been discovered and catalogued and are called rolling-pin limit cycles. The set exists for second-order feedback sections with two quantizers that round sign-magnitude or twos-complement products. The limit cycles are completely defined by three integers K, L, and M, and a simple construction rule. The peak amplitude approaches three times Jackson's peak estimate. The limit cycles exist for $B_1 - B_2$ pairs lying within rectangular regions in the $B_1 - B_2$ plane. They occur often in filters with high Q poles near dc or half the sampling frequency.

Specialized techniques requiring extra circuitry can be used to suppress rolling-pin limit cycles. These special techniques may also increase the roundoff noise in the presence of a signal. Alternately, these limit cycles may be avoided by making small changes in the binary coefficient values to produce a pair of coefficients just outside the region of existence of rolling-pin limit cycles and yet meet specified filter characteristics.

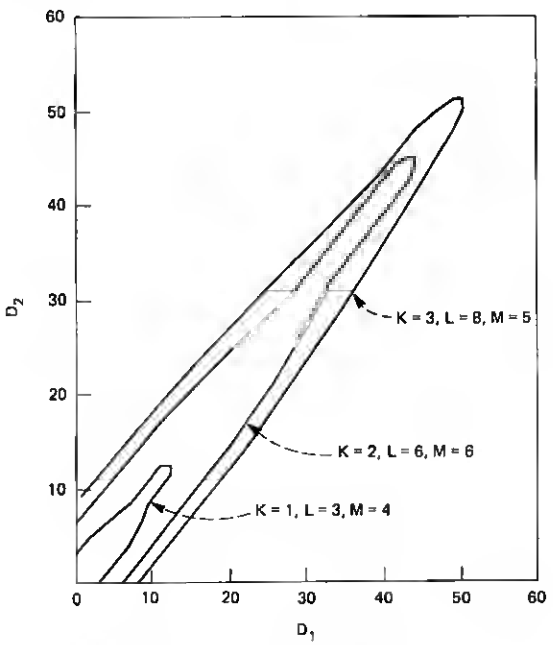

Fig. 19—Successive value plot for generalized K, L, M limit cycles.

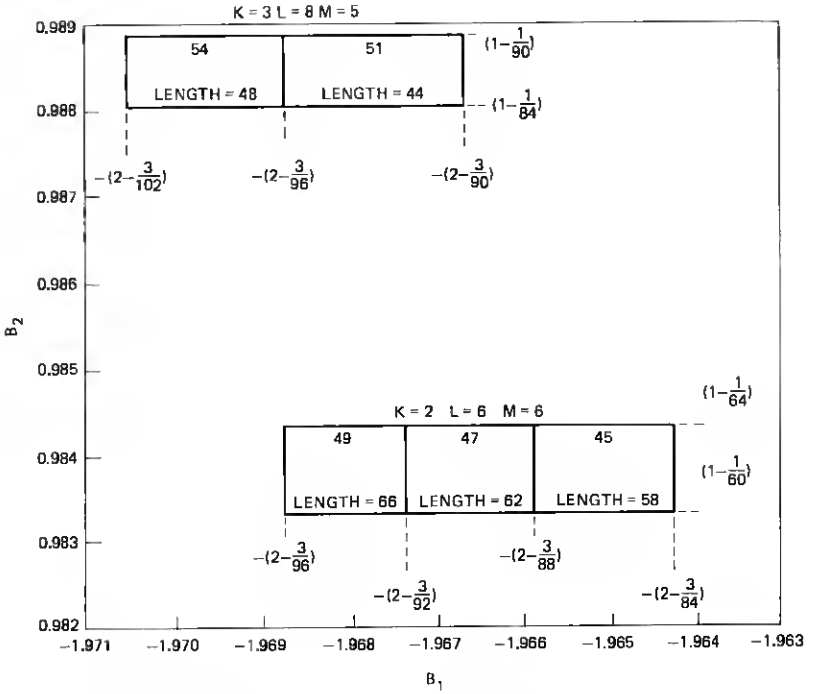

Fig. 20—Region of existence of generalized K, L, M limit cycles.

At present, these limit cycles are the largest (relative to Jackson's estimate) known in the region of the $B_1 - B_2$ plane where $|B_1| > 1.875$. For other regions, relatively large limit cycles have been found, but not systematized. It is expected that an approach similar to that presented will be useful. Other potentially useful extensions are for the cases of one quantizer and of truncation of products.

At present, these results can be useful to digital filter designers, whenever poles with $|B_1| > 1.875$ occur. Each design problem must be individually examined, however. A desirable goal is to incorporate these results into an automated design technique.

REFERENCES

1. S. L. Freeny, "Special-Purpose Hardware For Digital Filtering," Proc, IEEE, *63*, No. 4 (April 1975), pp. 633–648.
2. M. Buttner, "A Novel Approach to Eliminate Limit Cycles in Digital Filters with a Minimum Increase in the Quantization Noise," IEEE Trans. on Circuits and Systems, *CAS-24*, No. 6 (June 1977), pp. 300–304.
3. R. B. Kieburtz, V. B. Lawrence, and K. V. Mina, "Control of Limit Cycles in Recursive Digital Filters by Randomized Quantization," IEEE Trans. on Circuits and Systems, *CAS-24*, No. 6 (June 1977), pp. 291–299.
4. V. B. Lawrence and K. V. Mina, "Control of Limit Cycle Oscillations in Second Order Recursive Digital Filters using Constrained Random Truncation," IEEE Trans. on Acoustics, Speech and Signal Processing, *ASSP-26*, No. 2 (April 1978), pp. 127–134.

5. H. Butterweck, "Suppression of Parasitic Oscillations in Second Order Digital Filters by Means of a Controlled Rounding Arithmetic," AEU, *29* (December 1975), pp. 371–374.
6. Debasis Mitra and V. B. Lawrence, "Summary of Results on Controlled Rounding Arithmetics, For Direct Form Digital Filters, that Eliminate All Self-Sustained Oscillations," 1978 IEEE International Symposium on Circuits and Systems Proc., pp. 1023–1028.
7. L. B. Jackson, "An Analysis of Roundoff Noise in Digital Filters," Sc.D. Thesis, Stevens Institute of Technology, Hoboken, New Jersey, 1969.
8. S. R. Parker and S. F. Hess, "Limit Cycle Oscillations in Digital Filters," IEEE Trans. Circuit Theory, *CT-18*, No. 6 (November 1971), pp. 687–697.
9. I. W. Sandberg and J. F. Kaiser, "A Bound on Limit Cycles in Fixed-Point Implementations of Digital Filters," IEEE Trans. Audio and Electroacoustics, *AU-20*, No. 2 (June 1972), pp. 110–112.
10. J. L. Long and T. N. Trick, "An Absolute Bound on Limit Cycles due to Roundoff Errors in Digital Filters," IEEE Trans. Audio and Electroacoustics, *AU-21*, No. 1 (February 1973), pp. 27–30.
11. S. R. Parker and S. Yakowitz, "Computation of Bounds for Digital Filter Quantization Errors," IEEE Trans. Circuit Theory, *CT-20*, No. 4 (July 1973), pp. 391–396.
12. T. A. Claasen, W. Mecklenbrauker, and J. B. Peek, "Some Remarks on the Classification of Limit Cycles in Digital Filters," Phillips Research Reports, *28*, No. 4 (August 1973), pp. 297–303.